

KV-Embedding: Training-free Text Embedding via Internal KV Re-routing in Decoder-only LLMs

Yixuan Tang and Yi Yang

The Hong Kong University of Science and Technology

ytangch@connect.ust.hk, imyiyang@ust.hk

Abstract

While LLMs are powerful embedding backbones, their application in training-free settings faces two structural challenges: causal attention restricts early tokens from accessing subsequent context, and the next-token prediction objective biases representations toward generation rather than semantic compression. To address these limitations, we propose KV-Embedding, a framework that activates the latent representation power of frozen LLMs. Our method leverages the observation that the key-value (KV) states of the final token at each layer encode a compressed view of the sequence. By re-routing these states as a prepended prefix, we enable all tokens to access sequence-level context within a single forward pass. To ensure model-agnostic applicability, we introduce an automated layer selection strategy based on intrinsic dimensionality. Evaluations on MTEB across Qwen, Mistral, and Llama backbones show that KV-Embedding outperforms existing training-free baselines by up to 10%, while maintaining robust performance on sequences up to 4,096 tokens. These results demonstrate that internal state manipulation offers an efficient alternative to input modification, and we hope this work encourages further exploration of LLM internals for representation learning.

1 Introduction

Text embeddings power a wide range of NLP applications, from semantic search to retrieval-augmented generation (Lewis et al., 2020; Song et al., 2025). Recent work has shown that decoder-only LLMs can serve as strong embedding backbones when fine-tuned with contrastive objectives (Wang et al., 2024; BehnamGhader et al., 2024). However, these methods require substantial computational resources and large-scale datasets for each new backbone, limiting their scalability to rapidly evolving model architectures.

An appealing alternative is training-free embedding extraction: obtaining representations di-

rectly from frozen LLMs. This setting requires no optimization and applies immediately to any new model. However, two structural properties of decoder-only LLMs pose significant challenges. First, causal attention restricts each token to attend only to preceding positions, creating an information asymmetry where early tokens remain unaware of subsequent context (Springer et al., 2025). Second, the next-token prediction objective biases the final token toward predicting future content rather than distilling the semantic essence of the input (Jiang et al., 2024). Consequently, standard pooling strategies either average over incomplete representations (mean pooling) or rely on a prediction-biased vector (last-token pooling). For example, consider the phrase “the bank of the river”: due to the causal mask, the representation of “bank” is computed without knowledge of “river” and is thus inherently ambiguous. Since mean pooling aggregates all token states equally, this ambiguous representation degrades the quality of the final embedding.

Existing training-free methods address these limitations through various strategies. To mitigate the prediction bias, PromptEOL (Jiang et al., 2024) uses specially designed prompts to guide the final token toward semantic representation. To address information asymmetry, Echo (Springer et al., 2025) uses input repetition, while token prepending (Fu et al., 2025) inserts special tokens, both aiming to provide each token with global context. However, both Echo and token prepending rely on input-level modifications, which introduce their own limitations: input repetition doubles the sequence length, leading to a quadratic increase in attention complexity and potential “lost-in-the-middle” effects (Liu et al., 2024); token prepending relies on special tokens outside the model’s vocabulary, leading to unpredictable representations.

We take a different approach. Rather than reconstructing global context through input-level modi-

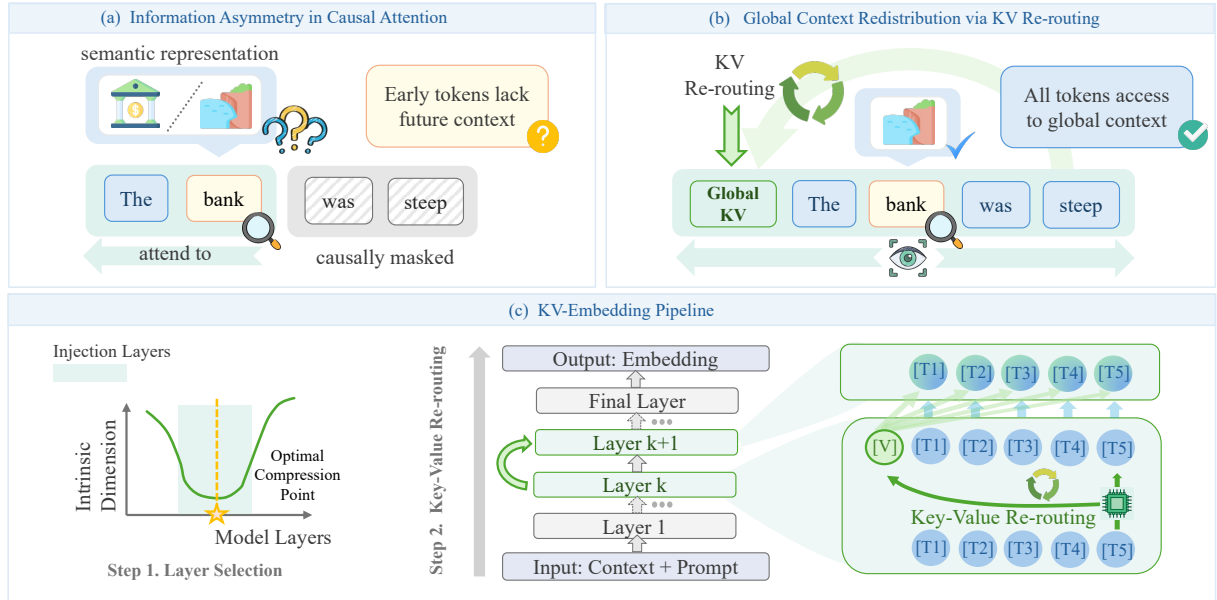


Figure 1: Overview of KV-Embedding. (a) Standard causal attention creates information asymmetry, as tokens only attend to preceding context. (b) KV-Embedding re-routes the last KV pair as a global prefix, enabling sequence-wide context access within one forward pass. (c) The pipeline identifies optimal re-routing anchors by locating layers with minimum intrinsic dimensionality, ensuring model-agnostic stability without manual tuning.

fications, we observe that the model already computes such global information internally. Specifically, the final token’s hidden state at each layer aggregates information from all preceding positions due to the causal attention structure (Radford et al., 2019). This raises a natural question: *can we directly leverage these internally computed global representations to produce higher-quality text embeddings?*

To this end, we propose **KV-Embedding**, a training-free framework that re-routes the Key and Value (KV) states of the final token as an internal prefix. As illustrated in Figure 1, the final token’s KV pair at each layer encodes that layer’s compressed view of the sequence (Katharopoulos et al., 2020; Geva et al., 2021). By prepending this pair to the attention mechanism, we enable all tokens to access a global summary within a single forward pass. We also adopt a prompt-based strategy to mitigate prediction bias in the final token. This design achieves sequence-wide context access without doubling the sequence length or introducing out-of-vocabulary tokens.

We further introduce an intrinsic dimensionality-based layer selection strategy to ensure model-agnostic applicability. Rather than performing re-routing at every layer, we identify layers where representations exhibit maximal compression, corresponding to points where the latent manifold di-

mensionality is minimized. By targeting these layers as re-routing anchors, we avoid interfering with early-layer feature extraction or late-layer prediction heads, ensuring that the redistributed context aligns with the model’s internal geometry.

Evaluations on MTEB (Muennighoff et al., 2023) and the long-context retrieval benchmark LoCoV1 (Saad-Falcon et al., 2024) demonstrate the efficacy of KV-Embedding. On MTEB, the proposed framework outperforms existing training-free methods by up to 10% across three backbones: Qwen3-4B (Yang et al., 2025), Mistral-7B (Jiang et al., 2023), and Llama-3.1-8B (Dubey et al., 2024). On LoCoV1, KV-Embedding maintains robust performance for sequences up to 4,096 tokens, where baseline methods degrade due to context dilution. Further analysis confirms that our method yields a more isotropic embedding space with improved alignment and uniformity.

In summary, KV-Embedding establishes a new state-of-the-art for training-free text embeddings through internal KV re-routing. The framework maintains model-agnostic applicability via automated layer selection based on intrinsic dimensionality, eliminating manual cross-architecture tuning. Extensive evaluations demonstrate that KV-Embedding provides an efficient and scalable solution for leveraging LLMs as text embedding models.

2 Related Work

The proposed framework builds upon three research directions: LLM-based text embeddings, training-free representation extraction, and internal state manipulation within the attention mechanism.

LLM-based Text Embeddings Text embedding has evolved from encoder-based models to decoder-only LLMs. Early explorations such as SGPT (Muennighoff, 2022) utilized position-weighted pooling, while subsequent models like E5-Mistral (Wang et al., 2024) and GTE (Li et al., 2023) achieved state-of-the-art results through contrastive fine-tuning on large-scale synthetic datasets. To overcome the inherent limitations of causal masking, LLM2Vec (BehnamGhader et al., 2024) and NV-Embed (Lee et al., 2025) modify the attention mask during training to enable bidirectional context. GritLM (Muennighoff et al., 2025) further unifies generative and embedding capabilities within a single architecture. While these training-based methods yield strong representations, the requirement for extensive computational resources and specialized datasets limits their scalability to the rapidly expanding landscape of LLMs. This motivates the development of training-free approaches that can leverage new models without additional optimization. Our work falls into this category, focusing on unlocking the representational capacity of frozen LLMs through internal state manipulation.

Training-Free LLM Embeddings Training-free methods aim to extract high-quality embeddings from frozen LLMs without parameter updates. However, this setting is constrained by the structural properties of decoder-only architectures: the next-token prediction objective biases final states toward future predictions rather than semantic summarization (Jiang et al., 2024), and causal attention creates an information asymmetry that leaves early tokens unaware of subsequent context (Springer et al., 2025). To address the former, PromptEOL (Jiang et al., 2024) and MetaEOL (Lei et al., 2024) design specific prompts to guide the model toward semantic compression. To address the latter, Echo (Springer et al., 2025) repeats the input sequence to simulate bidirectionality, though at the cost of doubling the sequence length. Token Prepending (Fu et al., 2025) mitigates this overhead by propagating auxiliary tokens, but relies on out-of-vocabulary tokens that may lead to unpre-

dictable representations. In contrast, our method redistributes internal states within the model’s native attention mechanism, enabling sequence-wide context access without modifying the input or introducing external tokens.

KV Manipulation in Attention In the Transformer architecture, the interaction between Query, Key, and Value determines the information flow across the sequence (Vaswani et al., 2017). Recent interpretability studies suggest that KV pairs function as a form of associative memory, where Keys encode addressing patterns and Values store semantic content (Geva et al., 2021). Research on information flow further indicates that global context accumulates within the KV states of specific anchor tokens during forward propagation (Wang et al., 2023). This provides a natural entry point for internal state manipulation. Prefix tuning (Li and Liang, 2021) prepends learnable KV pairs as a parameter-efficient fine-tuning strategy, while KV cache compression methods like StreamingLLM (Xiao et al., 2024) and H2O (Zhang et al., 2023) selectively retain entries to optimize inference efficiency. These approaches either require training or target generative throughput. In contrast, KV-Embedding leverages KV manipulation for representation extraction. By re-routing the final token’s KV states as a prefix within selected layers, our framework enables early tokens to access a compressed sequence summary, resolving the causal attention limitation within a single forward pass.

3 Method

We present KV-Embedding, a training-free framework for extracting high-quality text embeddings from decoder-only LLMs. The pipeline is illustrated in Figure 1.

3.1 Preliminaries

Given an input sequence $X = (x_1, \dots, x_n)$, a decoder-only LLM produces hidden states $\mathbf{h}_i^{(l)} \in \mathbb{R}^d$ through L sequential layers. For each layer l , the hidden state $\mathbf{h}_i^{(l)}$ is computed via multi-head causal self-attention. For simplicity, we describe the single-head case:

$$\mathbf{h}_i^{(l)} = \text{Attention} \left(\mathbf{q}_i^{(l)}, \mathbf{K}_{\leq i}^{(l)}, \mathbf{V}_{\leq i}^{(l)} \right) \quad (1)$$

where $\mathbf{K}_{\leq i}^{(l)} = [\mathbf{k}_1^{(l)}, \dots, \mathbf{k}_i^{(l)}]$ and $\mathbf{V}_{\leq i}^{(l)} = [\mathbf{v}_1^{(l)}, \dots, \mathbf{v}_i^{(l)}]$ denote the Key and Value matrices

from preceding positions. This causal constraint ensures that each \mathbf{h}_i is computed without visibility into subsequent tokens $x_{j>i}$. To extract a fixed-size embedding \mathbf{e} from a frozen LLM, a pooling function is applied to the final-layer hidden states:

$$\mathbf{e} = \text{Norm} \left(P \left(\mathbf{h}_1^{(L)}, \dots, \mathbf{h}_n^{(L)} \right) \right) \quad (2)$$

where $P(\cdot)$ denotes the pooling strategy and $\text{Norm}(\cdot)$ represents ℓ_2 normalization.

3.2 KV-Embedding

KV-Embedding addresses the structural limitations of causal attention through three components: a compression-oriented prompt, an internal KV re-routing mechanism, and an automated layer selection strategy.

3.2.1 Compression-Oriented Prompting

To mitigate the inherent next-token prediction bias, we wrap the input text in a template designed to trigger semantic compression:

“{Context/Query}: {text}” Compress the {Context/Query} in one word:

The prefix is set as “Context” for documents and “Query” for queries. This template leverages the model’s generation capability to guide the final token representation \mathbf{h}_n toward distilling the semantic essence of the input.

3.2.2 Key-Value Re-Routing

While prompting shapes the optimization target, it does not resolve the unidirectional information flow: early tokens still cannot access subsequent context. We address this by re-routing the KV states of the final token as a global prefix within each selected layer.

At each layer $l \in \mathcal{L}$, we first compute the Key and Value projections for all positions, yielding the full matrices $\mathbf{K}^{(l)}$ and $\mathbf{V}^{(l)}$. We then extract the KV pair at the final position $(\mathbf{k}_n^{(l)}, \mathbf{v}_n^{(l)})$, which encodes that layer’s aggregated view of the sequence due to the causal structure. This pair is prepended to the KV matrices before computing attention:

$$\begin{aligned} \tilde{\mathbf{K}}_{\leq i}^{(l)} &= \left[\mathbf{k}_n^{(l)} \parallel \mathbf{K}_{\leq i}^{(l)} \right] \\ \tilde{\mathbf{V}}_{\leq i}^{(l)} &= \left[\mathbf{v}_n^{(l)} \parallel \mathbf{V}_{\leq i}^{(l)} \right] \end{aligned} \quad (3)$$

where \parallel denotes concatenation along the sequence dimension. This operation is applied independently

to each attention head. The augmented matrices allow every query \mathbf{q}_i to attend to the global summary at virtual position 0, enabling early tokens to access sequence-level context within a single forward pass. Both components are essential: the key enables content-based addressing, while the value carries the aggregated semantic information. We empirically verify that the final token’s KV states capture sequence-level semantics through probing experiments in Appendix B. The complete algorithm is provided in Appendix A. We further introduce an attention bias b added to the pre-softmax logits when attending to the re-routed position, controlling how strongly each token attends to the global summary. We set $b = 1.0$ based on ablation studies. Detailed formulation is provided in Appendix G.

3.2.3 Automated Layer Selection via Intrinsic Dimensionality

The functional specialization of layers necessitates careful selection of the re-routing set \mathcal{L} . Shallow layers encode surface-level patterns while final layers are biased toward vocabulary prediction (Skean et al., 2025). To identify layers with high semantic density, we leverage Intrinsic Dimensionality (ID), following the observation that the ID minimum corresponds to maximal semantic abstraction (Valeriani et al., 2023). We observe that ID trajectories vary by architecture (see Appendix I), necessitating an adaptive selection strategy.

We employ the TwoNN estimator (Facco et al., 2017) to compute ID across layers using 1,000 sentences from F2LLM (Zhang et al., 2025). For models exhibiting a clear U-shaped trajectory, we identify the layer l^* achieving minimum ID and define:

$$\mathcal{L} = \{l \mid l^* \leq l \leq \min(L, l^* + \lfloor 0.1L \rfloor)\} \quad (4)$$

This yields a contiguous window starting from the compression peak. For models with multiple local minima, we instead select layers from low-ID regions in the middle-to-late portion of the network, excluding the first $\lfloor 0.2L \rfloor$ layers that primarily encode surface features. This strategy targets layers where representations are most compressed while avoiding early-layer noise and late-layer prediction bias. We provide empirical validation in Appendix C.

Finally, the sequence embedding \mathbf{e} is obtained by averaging mean pooling and last-token pooling over the final-layer hidden states, combining distributional evidence across positions with the

globally-informed final state, followed by ℓ_2 normalization.

4 Experiments

In this section, we evaluate KV-Embedding across multiple benchmarks and model architectures to demonstrate its efficacy as a training-free framework for generating high-quality text representations.

4.1 Experimental Setup

Benchmarks. We evaluate KV-Embedding on two complementary benchmarks. MTEB (Muenninghoff et al., 2023) provides a multi-task assessment across seven categories: STS, Retrieval, Classification, Pair Classification, Clustering, Reranking, and Summarization. To evaluate robustness in long-context scenarios, we use LoCoV1 (Saad-Falcon et al., 2024), truncating documents to 1024, 2048, and 4096 tokens. This provides a stress test for KV re-routing, as causal attention typically suffers from context dilution in long sequences. Detailed task descriptions and dataset statistics for these benchmarks are provided in Appendix D.

Models. To demonstrate the model-agnostic nature of our approach, we experiment with three widely-used decoder-only LLMs covering different parameter scales and families: Qwen3-4B (Yang et al., 2025), Mistral-7B-Instruct-v0.1 (Jiang et al., 2023), and Llama-3.1-8B-Instruct (Dubey et al., 2024). All evaluations are performed in a zero-shot, training-free setting.

Baselines. We compare KV-Embedding against representative training-free strategies. Last Token uses the final hidden state \mathbf{h}_n , while Mean Pooling averages all hidden states. PromptEOL (Jiang et al., 2024) guides semantic compression via a template prompt. Echo (Springer et al., 2025) repeats the input sequence to simulate bidirectionality, doubling the sequence length. Token Prepending (Fu et al., 2025) propagates context via special tokens, starting from layer 8 and extracting representations from the 6th-to-final layer. We also report an ablation (w/o KV Re-routing) that uses our prompt and pooling strategy but disables the key-value re-routing component. All methods extract representations from the final layer unless otherwise specified.

Implementation. We estimate intrinsic dimensionality via TwoNN (Facco et al., 2017) on 1,000

sentences from F2LLM (Zhang et al., 2025). For Qwen3-4B and Mistral-7B-Instruct-v0.1, which exhibit clear ID minima in middle layers, we apply KV re-routing to contiguous regions: layers 12–21 for Qwen3-4B and layers 13–19 for Mistral-7B-Instruct-v0.1. Llama-3.1-8B shows a more complex trajectory with multiple local minima; we select layers from low-ID regions excluding the shallow minimum (layers 10–11, 20, 26–31). The maximum sequence length is 512 for MTEB. Experiments are conducted on 4 NVIDIA H800 GPUs with batch size 64 and random seed 42.

4.2 Results

Table 1 and Table 2 present average results on MTEB and LoCoV1 respectively. The detailed data are provided in the Appendix E and F.

MTEB Results. As shown in Table 1, KV-Embedding consistently outperforms all baselines across the three backbones. Compared to PromptEOL and Echo, our method achieves higher performance while maintaining the original sequence length. To disentangle the contributions of each component, we ablate KV re-routing while retaining the compression-oriented prompt. The ablation (w/o KV Re-routing) results in a performance drop across all models: on Mistral-7B, the average score decreases from 0.534 to 0.450. This confirms that while the prompt mitigates prediction bias, KV re-routing is the primary driver of improvement.

Impact Across Task Categories. Performance improvements vary by task type. Tasks requiring holistic semantic understanding show significant gains; notably, Retrieval exhibits the largest increase, reaching 0.2765 on Qwen3-4B compared to 0.1857 for PromptEOL. This suggests that document-level matching benefits from access to global information across the entire sequence. The ablation confirms this pattern: removing re-routing also causes the largest drop in Retrieval. STS and Clustering also show consistent improvements, while Summarization tasks show the smallest variance across methods, with all approaches performing within a similar range.

Long-Context Evaluation. Table 2 presents results on LoCoV1 across different sequence lengths. KV-Embedding substantially outperforms all baselines at every length tested. On Mistral-7B, our method achieves scores above 0.18 across all

Method	STS	Retr.	Class.	Pair.	Clust.	Rerank.	Summ.	Avg.
<i>Qwen3-4B</i>								
Last Token	0.2818	0.0722	0.4243	0.3054	0.2395	0.3476	0.2341	0.2721
Mean Pooling	0.4571	0.0294	0.4656	0.5269	0.3305	0.3272	0.1949	0.3331
PromptEOL	0.6741	0.1857	0.6138	0.5637	0.3651	0.4924	0.2396	0.4478
Echo	0.6634	0.1727	0.5761	0.6367	0.3530	0.4315	0.2294	0.4375
Token Prepending	0.6370	0.1622	0.6283	0.5206	0.3372	0.4901	0.2483	0.4320
KV-Embedding	0.7141	0.2765	0.6375	0.6800	0.3903	0.5007	0.2566	0.4937
<i>w/o KV Re-routing</i>	0.5631	0.2023	0.5094	0.5296	0.3769	0.4600	0.2257	0.4096
<i>Mistral-7B-Instruct-v0.1</i>								
Last Token	0.3915	0.1036	0.5314	0.3440	0.2516	0.3673	0.2823	0.3245
Mean Pooling	0.4885	0.0886	0.5157	0.5681	0.3472	0.3790	0.2557	0.3775
PromptEOL	0.6953	0.1746	0.6571	0.5629	0.3158	0.4835	0.2863	0.4537
Echo	0.7333	0.2414	0.6398	0.7560	0.3681	0.4751	0.2922	0.5008
Token Prepending	0.6775	0.1619	0.6580	0.5764	0.2825	0.4790	0.2921	0.4468
KV-Embedding	0.7720	0.3014	0.6951	0.7564	0.3902	0.5145	0.3088	0.5341
<i>w/o KV Re-routing</i>	0.6478	0.2014	0.6008	0.5931	0.3611	0.4804	0.2664	0.4502
<i>Llama-3.1-8B-Instruct</i>								
Last Token	0.3513	0.0887	0.4769	0.3554	0.2652	0.3608	0.2526	0.3073
Mean Pooling	0.4702	0.0713	0.4848	0.5176	0.3577	0.3537	0.1996	0.3507
PromptEOL	0.6919	0.2017	0.6250	0.5911	0.4035	0.4991	0.2788	0.4702
Echo	0.7124	0.2941	0.6261	0.7125	0.4189	0.5074	0.2527	0.5034
Token Prepending	0.6968	0.1817	0.6577	0.5734	0.3365	0.4992	0.2880	0.4619
KV-Embedding	0.7398	0.3079	0.6602	0.7332	0.4448	0.5237	0.2796	0.5270
<i>w/o KV Re-routing</i>	0.6187	0.2088	0.5611	0.5839	0.4076	0.5044	0.2746	0.4513

Table 1: Results on MTEB. Each data reports the main metric for the corresponding task category, averaged across datasets. KV-Embedding achieves the best overall performance across all backbones. *w/o KV Re-routing* ablates re-routing while retaining the compression prompt. The highest average score for each model is highlighted in **bold**.

settings, while baselines remain below 0.10 regardless of sequence length. Similar patterns hold for Qwen3-4B and Llama-3.1-8B, where KV-Embedding consistently outperforms the best baseline by a factor of 1.3–3.5 \times . These results suggest that baseline methods struggle with long-context retrieval in general, likely because the final token cannot effectively aggregate information from distant positions under causal attention. By explicitly re-routing a global summary to all positions, KV-Embedding enables more effective long-range information integration.

5 Analysis and Ablation

In this section, we conduct a series of experiments to explore the KV-Embedding framework, validate its core mechanisms, and analyze the resulting embedding space quality.

5.1 Mechanism Validation

Risks of Naive Mask Removal A natural question is whether simply removing the causal mask

can achieve global context access. As shown in Table 4, this approach fails: applying bidirectional attention consistently degrades performance, scoring even lower than the simple last-token baseline on both Qwen3-4B and Mistral-7B-Instruct-v0.1. This failure occurs because decoder-only LLMs are optimized for unidirectional patterns during pre-training; forcing tokens to attend to future positions introduces out-of-distribution states that the model cannot process effectively. In contrast, KV-Embedding relocates existing KV states rather than altering the attention structure, preserving the model’s internal manifold while resolving information asymmetry. Further analysis is provided in Appendix K.

5.2 Embedding Analysis

Attention Pattern Visualization Table 3 compares the attention distribution of the final token across different methods. Echo exhibits a strong recency bias, focusing primarily on the last tokens. PromptEOL and Token Prepending capture spe-

Method	1024	2048	4096
<i>Qwen3-4B</i>			
PromptEOL	0.0413	0.0438	0.1286
Echo	0.0961	0.0658	0.1318
Token Prepending	0.0414	0.0422	0.1255
KV-Embedding	0.1289	0.1192	0.1822
<i>Mistral-7B-Instruct-v0.1</i>			
PromptEOL	0.0414	0.0407	0.0442
Echo	0.0627	0.0549	0.0591
Token Prepending	0.0416	0.0422	0.0992
KV-Embedding	0.2165	0.1838	0.2068
<i>Llama-3.1-8B-Instruct</i>			
PromptEOL	0.0463	0.0410	0.1285
Echo	0.1128	0.0385	0.1191
Token Prepending	0.0421	0.0422	0.1397
KV-Embedding	0.2191	0.1817	0.2404

Table 2: Retrieval performance (NDCG@10) on Lo-CoV1 across different context lengths. KV-Embedding consistently outperforms all baselines regardless of sequence length.

cific keywords but often miss initial intent-bearing words like ‘‘Looking’’. In contrast, KV-Embedding demonstrates a more structured alignment with the query; it assigns higher weights to both the intent word ‘‘Looking’’ and functional anchors such as ‘‘examples’’ and ‘‘beginners’’. This pattern indicates that re-routing global context enables the final state to aggregate key semantic components from disparate positions, overcoming the limitations of causal attention.

Embedding Space Quality Table 5 presents the alignment and uniformity metrics (Wang and Isola, 2020) for Mistral-7B-Instruct. Alignment evaluates the proximity of embeddings for similar sentence pairs, while uniformity assesses the feature distribution on the hypersphere. KV-Embedding achieves the best values for both metrics compared to the baselines. The improvement in uniformity indicates that internal KV re-routing helps mitigate the anisotropy problem inherent in decoder-only LLMs, where representations tend to cluster within a narrow cone. By redistributing global context, KV-Embedding encourages a more discriminative and isotropic embedding space. Detailed experimental settings regarding the geometric analysis are provided in Appendix H.

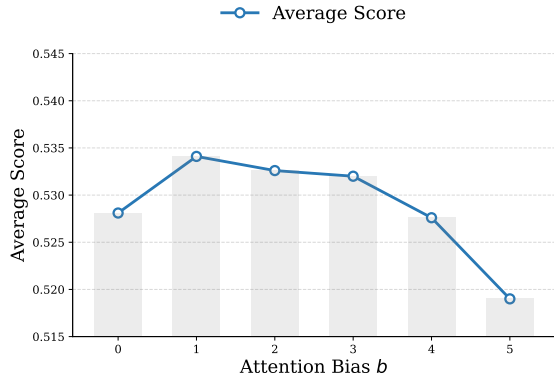


Figure 2: Average performance of Mistral-7B-Instruct with KV-Embedding across different attention bias values. A bias value of 1.0 corresponds to the highest average score.

5.3 Ablation of Key Components

Effect of Attention Bias We add an attention bias b to the pre-softmax logits when attending to the re-routed position, controlling how strongly each token attends to the global summary. As shown in Figure 2, performance improves from $b = 0$ to $b = 1.0$, confirming that the re-routed context directly enhances embedding quality. The curve remains stable across a wide range, suggesting that the injected KV pairs integrate naturally with the pre-trained attention mechanism. However, performance declines when $b > 3.0$, indicating over-reliance on the global summary. We set $b = 1.0$ to balance global context access with local specificity. Detailed formulation and full results are provided in Appendix G.

Effectiveness of ID-based Layer Selection We compare our ID-based strategy with uniform selection targeting the early, middle, or late thirds of the network. As detailed in Appendix J, re-routing at early layers yields the lowest performance (0.409 on Qwen3-4B), confirming that shallow representations lack the semantic density required for effective context redistribution. The ID-based strategy achieves the highest scores (0.494 on Qwen3-4B, 0.534 on Mistral-7B) while using fewer layers than uniform alternatives. On Mistral-7B, ID selection (7 layers) outperforms the 10-layer middle-third strategy, demonstrating that the ID minimum effectively identifies layers with peak semantic abstraction.

Pooling Strategy We evaluate the impact of different aggregation methods, including last-token, mean, and hybrid pooling. As shown in Ap-

Method	Key Tokens with Attention Weights
Echo	Looking for comprehensive machine learning tutorials that cover neural networks decision trees and deep learning algorithms with practical Python code examples suitable for beginners
PromptEOL	Looking for comprehensive machine learning tutorials that cover neural networks decision trees and deep learning algorithms with practical Python code examples suitable for beginners
Token Prepending	Looking for comprehensive machine learning tutorials that cover neural networks decision trees and deep learning algorithms with practical Python code examples suitable for beginners
KV-Embedding	Looking for comprehensive machine learning tutorials that cover neural networks decision trees and deep learning algorithms with practical Python code examples suitable for beginners

Table 3: Attention distribution for search query: “Looking for comprehensive machine learning tutorials that cover neural networks, decision trees, and deep learning algorithms with practical Python code examples suitable for beginners.” Colors represent attention weights (white: <0.012 , light: $0.012\text{--}0.055$, medium: $0.055\text{--}0.15$, dark: >0.15). Key content words are shown.

Model	Method	STS	Retr.	Clas.	Pair.	Clust.	Rerank.	Summ.	Avg.
Qwen3-4B	Last Token + Bi-Attn	0.1794	0.0248	0.3764	0.2214	0.1901	0.3146	0.2530	0.2228
	Last Token + Causal Attn	0.2818	0.0722	0.4243	0.3054	0.2395	0.3476	0.2341	0.2721
	KV-Embedding	0.7141	0.2765	0.6375	0.6800	0.3903	0.5007	0.2566	0.4937
Mistral-7B-Instruct	Last Token + Bi-Attn	0.2255	0.0216	0.4133	0.2748	0.2308	0.3458	0.2746	0.2552
	Last Token + Causal Attn	0.3915	0.1036	0.5314	0.3440	0.2516	0.3673	0.2823	0.3245
	KV-Embedding	0.7720	0.3014	0.6951	0.7564	0.3902	0.5145	0.3088	0.5341

Table 4: Impact of attention constraints. Removing the causal mask (Bi-Attn) causes performance collapse, while KV-Embedding enables global context access without violating causal priors.

Method	Alignment (↓)	Uniformity (↓)
PromptEOL	0.7378	-2.2715
Echo	0.6366	-2.0794
Token Prepending	0.7505	-2.2233
KV-Embedding	0.6082	-2.3899

Table 5: Alignment and uniformity analysis on Mistral-7B-Instruct-v0.1 with different methods. ↓ indicates lower is better.

pendix M, the hybrid strategy, which averages the representations from last-token and mean pooling, shows greater consistency across different models and tasks. Mean pooling tends to underperform, as it weights all tokens equally without prioritizing the globally-informed final state. Based on these findings, we adopt the hybrid approach in the main experiments.

Robustness to Prompt Design To evaluate sensitivity to prompt design, we test five templates varying in prefix and verb choice. Performance remains within a narrow range (0.529–0.540), as shown in Appendix L. This stability suggests that KV-Embedding is relatively insensitive to prompt variations, and that internal KV re-routing may reduce the reliance on specific instructions to elicit

semantic representations.

6 Conclusion

We introduced KV-Embedding, a training-free framework that extracts text representations from decoder-only LLMs by redistributing their internal states. By re-routing the final token’s KV states as a prefix within selected layers, our approach enables all positions to access a compressed sequence summary within a single forward pass, effectively addressing the information asymmetry inherent in causal attention. An automated layer selection strategy based on intrinsic dimensionality enables model-agnostic applicability without manual tuning. Evaluations on MTEB and the long-context retrieval benchmark LoCoV1 demonstrate that KV-Embedding outperforms existing training-free methods by up to 10%, while maintaining robust performance on sequences up to 4,096 tokens. These results suggest that decoder-only LLMs contain latent representational capacity that can be unlocked through internal state manipulation rather than external input modification. We hope this work encourages further exploration of internal mechanisms in LLMs, bridging the gap between generative pretraining and representation learning.

Limitations

Despite the consistent improvements of KV-Embedding over training-free baselines, two main limitations should be noted. First, the re-routing mechanism increases latency compared to standard pooling. Second, as a training-free method, KV-Embedding may not match the performance of supervised models fine-tuned with contrastive objectives on large datasets. Therefore, it can serve as a practical alternative for resource-constrained scenarios rather than a full replacement for state-of-the-art supervised text embeddings.

References

Parishad BehnamGhader, Vaibhav Adlakha, Marius Mosbach, Dzmitry Bahdanau, Nicolas Chapados, and Siva Reddy. 2024. LLM2vec: Large language models are secretly powerful text encoders. In *First Conference on Language Modeling*.

Abhimanyu Dubey, Abhinav Jauhri, Abhinav Pandey, Abhishek Kadian, Ahmad Al-Dahle, Aiesha Letman, Akhil Mathur, Alan Schelten, Amy Yang, Angela Fan, and 1 others. 2024. The llama 3 herd of models. *arXiv e-prints*, pages arXiv–2407.

Elena Facco, Maria d’Errico, Alex Rodriguez, and Alessandro Laio. 2017. Estimating the intrinsic dimension of datasets by a minimal neighborhood information. *Scientific reports*, 7(1):12140–8.

Yuchen Fu, Zifeng Cheng, Zhiwei Jiang, Zhonghui Wang, Yafeng Yin, Zhengliang Li, and Qing Gu. 2025. Token prepending: A training-free approach for eliciting better sentence embeddings from llms. In *Proceedings of the 63rd Annual Meeting of the Association for Computational Linguistics (Volume 1: Long Papers)*, ACL 2025, pages 3168–3181. Association for Computational Linguistics.

Mor Geva, Roei Schuster, Jonathan Berant, and Omer Levy. 2021. Transformer feed-forward layers are key-value memories. In *Proceedings of the 2021 Conference on Empirical Methods in Natural Language Processing, EMNLP 2021*, pages 5484–5495. Association for Computational Linguistics.

Albert Q. Jiang, Alexandre Sablayrolles, Arthur Mensch, Chris Bamford, Devendra Singh Chaplot, Diego de las Casas, Florian Bressand, Gianna Lengyel, Guillaume Lample, Lucile Saulnier, Lélio Renard Lavaud, Marie-Anne Lachaux, Pierre Stock, Teven Le Scao, Thibaut Lavril, Thomas Wang, Timothée Lacroix, and William El Sayed. 2023. *Mistral 7b*. Preprint, arXiv:2310.06825.

Ting Jiang, Shaohan Huang, Zhongzhi Luan, Deqing Wang, and Fuzhen Zhuang. 2024. Scaling sentence embeddings with large language models. In *Findings of the Association for Computational Linguistics: EMNLP*, pages 3182–3196. Association for Computational Linguistics.

Angelos Katharopoulos, Apoorv Vyas, Nikolaos Papas, and François Fleuret. 2020. Transformers are rnns: Fast autoregressive transformers with linear attention. In *Proceedings of the 37th International Conference on Machine Learning, ICML 2020*, volume 119 of *Proceedings of Machine Learning Research*, pages 5156–5165. PMLR.

Chankyu Lee, Rajarshi Roy, Mengyao Xu, Jonathan Raiman, Mohammad Shoeybi, Bryan Catanzaro, and Wei Ping. 2025. Nv-embed: Improved techniques for training llms as generalist embedding models. In *The Thirteenth International Conference on Learning Representations, ICLR 2025*. OpenReview.net.

Yibin Lei, Di Wu, Tianyi Zhou, Tao Shen, Yu Cao, Chongyang Tao, and Andrew Yates. 2024. Meta-task prompting elicits embeddings from large language models. In *Proceedings of the 62nd Annual Meeting of the Association for Computational Linguistics (Volume 1: Long Papers)*, ACL 2024, pages 10141–10157. Association for Computational Linguistics.

Patrick Lewis, Ethan Perez, Aleksandra Piktus, Fabio Petroni, Vladimir Karpukhin, Naman Goyal, Heinrich Küttler, Mike Lewis, Wen-tau Yih, Tim Rocktäschel, Sebastian Riedel, and Douwe Kiela. 2020. Retrieval-augmented generation for knowledge-intensive NLP tasks. In *Advances in Neural Information Processing Systems 33: Annual Conference on Neural Information Processing Systems 2020, NeurIPS 2020, December 6–12, 2020, virtual*.

Xiang Lisa Li and Percy Liang. 2021. Prefix-tuning: Optimizing continuous prompts for generation. In *Proceedings of the 59th Annual Meeting of the Association for Computational Linguistics and the 11th International Joint Conference on Natural Language Processing, ACL/IJCNLP 2021, (Volume 1: Long Papers)*, pages 4582–4597. Association for Computational Linguistics.

Zehan Li, Xin Zhang, Yanzhao Zhang, Dingkun Long, Pengjun Xie, and Meishan Zhang. 2023. Towards general text embeddings with multi-stage contrastive learning. *CoRR*, abs/2308.03281.

Nelson F. Liu, Kevin Lin, John Hewitt, Ashwin Paranjape, Michele Bevilacqua, Fabio Petroni, and Percy Liang. 2024. Lost in the middle: How language models use long contexts. *Transactions of the Association for Computational Linguistics*, 12:157–173.

Niklas Muennighoff. 2022. SGPT: GPT sentence embeddings for semantic search. *CoRR*, abs/2202.08904.

Niklas Muennighoff, Hongjin Su, Liang Wang, Nan Yang, Furu Wei, Tao Yu, Amanpreet Singh, and Douwe Kiela. 2025. Generative representational instruction tuning. In *The Thirteenth International Conference on Learning Representations, ICLR 2025*. OpenReview.net.

Niklas Muennighoff, Nouamane Tazi, Loic Magne, and Nils Reimers. 2023. MTEB: Massive text embedding benchmark. In *Proceedings of the 17th Conference of the European Chapter of the Association for Computational Linguistics*, pages 2014–2037. Association for Computational Linguistics.

Alec Radford, Jeffrey Wu, Rewon Child, David Luan, Dario Amodei, Ilya Sutskever, and 1 others. 2019. Language models are unsupervised multitask learners. *OpenAI blog*, 1(8):9.

Jon Saad-Falcon, Daniel Y. Fu, Simran Arora, Neel Guha, and Christopher Ré. 2024. Benchmarking and building long-context retrieval models with loco and m2-bert. In *Proceedings of the 41st International Conference on Machine Learning*, ICML’24. JMLR.org.

Oscar Skean, Md Rifat Arefin, Dan Zhao, Niket Nikul Patel, Jalal Naghiyev, Yann LeCun, and Ravid Shwartz-Ziv. 2025. Layer by layer: Uncovering hidden representations in language models. In *Forty-second International Conference on Machine Learning*.

Tingyu Song, Guo Gan, Mingsheng Shang, and Yilun Zhao. 2025. IFIR: A comprehensive benchmark for evaluating instruction-following in expert-domain information retrieval. In *Proceedings of the 2025 Conference of the Nations of the Americas Chapter of the Association for Computational Linguistics: Human Language Technologies, NAACL 2025 - Volume 1: Long Papers, Albuquerque, New Mexico, USA, April 29 - May 4, 2025*, pages 10186–10204. Association for Computational Linguistics.

Jacob Mitchell Springer, Suhas Kotha, Daniel Fried, Graham Neubig, and Aditi Raghunathan. 2025. Repetition improves language model embeddings. In *The Thirteenth International Conference on Learning Representations, ICLR 2025*. OpenReview.net.

Lucrezia Valeriani, Diego Doimo, Francesca Cuturello, Alessandro Laio, Alessio Ansuini, and Alberto Cazzaniga. 2023. The geometry of hidden representations of large transformer models. In *Advances in Neural Information Processing Systems 36: Annual Conference on Neural Information Processing Systems 2023, NeurIPS 2023*.

Ashish Vaswani, Noam Shazeer, Niki Parmar, Jakob Uszkoreit, Llion Jones, Aidan N. Gomez, Łukasz Kaiser, and Illia Polosukhin. 2017. Attention is all you need. In *Advances in Neural Information Processing Systems 30: Annual Conference on Neural Information Processing Systems 2017*, pages 5998–6008.

Lean Wang, Lei Li, Damai Dai, Deli Chen, Hao Zhou, Fandong Meng, Jie Zhou, and Xu Sun. 2023. Label words are anchors: An information flow perspective for understanding in-context learning. In *Proceedings of the 2023 Conference on Empirical Methods in Natural Language Processing, EMNLP 2023*, pages 9840–9855. Association for Computational Linguistics.

Liang Wang, Nan Yang, Xiaolong Huang, Linjun Yang, Rangan Majumder, and Furu Wei. 2024. Improving text embeddings with large language models. In *Proceedings of the 62nd Annual Meeting of the Association for Computational Linguistics (Volume 1: Long Papers), ACL 2024*, pages 11897–11916. Association for Computational Linguistics.

Tongzhou Wang and Phillip Isola. 2020. Understanding contrastive representation learning through alignment and uniformity on the hypersphere. In *Proceedings of the 37th International Conference on Machine Learning, ICML 2020*, volume 119 of *Proceedings of Machine Learning Research*, pages 9929–9939. PMLR.

Guangxuan Xiao, Yuandong Tian, Beidi Chen, Song Han, and Mike Lewis. 2024. Efficient streaming language models with attention sinks. In *The Twelfth International Conference on Learning Representations, ICLR 2024*. OpenReview.net.

An Yang, Anfeng Li, Baosong Yang, Beichen Zhang, Binyuan Hui, Bo Zheng, Bowen Yu, Chang Gao, Chengan Huang, Chenxu Lv, and 1 others. 2025. Qwen3 technical report. *arXiv preprint arXiv:2505.09388*.

Zhenyu Zhang, Ying Sheng, Tianyi Zhou, Tianlong Chen, Lianmin Zheng, Ruisi Cai, Zhao Song, Yuandong Tian, Christopher Ré, Clark W. Barrett, Zhangyang Wang, and Beidi Chen. 2023. H2O: heavy-hitter oracle for efficient generative inference of large language models. In *Advances in Neural Information Processing Systems 36: Annual Conference on Neural Information Processing Systems 2023, NeurIPS 2023*.

Ziyin Zhang, Zihan Liao, Hang Yu, Peng Di, and Rui Wang. 2025. F2LLM technical report: Matching SOTA embedding performance with 6 million open-source data. *CoRR*, abs/2510.02294.

A Algorithm Details

Algorithm 1 summarizes the complete KV-Embedding procedure. The method requires only a single forward pass, with KV re-routing applied at the selected layers \mathcal{L} .

B Probing KV States for Sequence Information

To empirically verify that the final token’s KV states capture richer sequence-level semantics than earlier positions, we conduct a probing experiment on text classification tasks.

Algorithm 1 KV-Embedding

Require: Text x , LLM with L layers, layer set \mathcal{L}
Ensure: Embedding e

- 1: Apply compression prompt to x
- 2: **for** $l = 1, \dots, L$ **do**
- 3: $\mathbf{K}^{(l)}, \mathbf{V}^{(l)} \leftarrow$ key-value projections
- 4: **if** $l \in \mathcal{L}$ **then**
- 5: $\mathbf{k}_n, \mathbf{v}_n \leftarrow$ KV at final position
- 6: $\tilde{\mathbf{K}}^{(l)} \leftarrow [\mathbf{k}_n \parallel \mathbf{K}^{(l)}]$
- 7: $\tilde{\mathbf{V}}^{(l)} \leftarrow [\mathbf{v}_n \parallel \mathbf{V}^{(l)}]$
- 8: Attention($\mathbf{Q}^{(l)}, \tilde{\mathbf{K}}^{(l)}, \tilde{\mathbf{V}}^{(l)}$)
- 9: **else**
- 10: Standard attention
- 11: **end if**
- 12: **end for**
- 13: $\mathbf{e}_1 \leftarrow \mathbf{h}_n^{(L)}, \mathbf{e}_2 \leftarrow \text{Mean}(\mathbf{H}^{(L)})$
- 14: **return** Normalize($(\mathbf{e}_1 + \mathbf{e}_2)/2$)

Setup We select two classification datasets from MTEB (Muennighoff et al., 2023): ImdbClassification (binary sentiment) and TweetSentimentExtractionClassification (three-way sentiment). For each dataset, we sample 1,000 training instances and 500 validation instances. We perform a forward pass through Mistral-7B-Instruct (Jiang et al., 2023) and extract KV states from three positions: the first token, the middle token, and the last token. For each position, we concatenate the key and value vectors across all attention heads at the final layer, yielding a fixed-dimensional representation. A logistic regression classifier is trained on these frozen representations, with the L2 regularization coefficient selected via cross-validation over the range $[10^{-4}, 10^1]$.

Results Table 6 presents the probing accuracy for each position. Across both datasets, the last token consistently achieves the highest accuracy. On IMDB, the accuracy improves from 51.4% at the first position to 85.2% at the last position, a gain of over 33 absolute points. A similar trend is observed on Tweet sentiment classification, where the last position outperforms the first by 15.6 points. These results confirm that sequence-level information progressively accumulates toward the end under causal attention, providing direct empirical support for our KV re-routing approach.

C Layer-wise Representation Analysis

To understand how representation quality evolves across layers and validate our layer selection strategy, we evaluate the last token’s hidden states at each layer on semantic similarity tasks using Mistral-7B-Instruct (Jiang et al., 2023).

Position	IMDB	TweetSentiment
First	51.4	45.2
Middle	73.0	52.6
Last	85.2	60.8

Table 6: Probing accuracy (%) on classification tasks using KV states from different token positions in Mistral-7B-Instruct.

Setup We extract hidden states from all 32 layers and evaluate on two tasks: Pair Classification, which measures fine-grained semantic matching via cosine AP, and STS, which measures similarity via Spearman correlation. These tasks reveal complementary aspects of representation quality.

Results Table 7 reveals distinct patterns for the two tasks. Pair Classification peaks at layers 10–13 and declines thereafter, indicating that middle layers capture the most discriminative features for fine-grained semantic matching. In contrast, STS improves toward later layers, likely due to the next-token prediction bias that emphasizes local word associations over holistic semantics.

Layer Range	Pair Class.	STS
0–6	0.270	0.221
7–12	0.302	0.282
13–19 (ID-selected)	0.301	0.290
20–26	0.286	0.297
27–32	0.275	0.339

Table 7: Layer-wise probing performance on Mistral-7B-Instruct. The ID-selected range maintains strong average performance while avoiding the generation-biased later layers.

Our ID-based strategy selects layers 13–19, corresponding to a transition zone where semantic abstraction is high but prediction bias has not yet dominated. This range avoids early layers with insufficient semantic content and final layers increasingly optimized for next-token prediction. The Pair Classification results support this choice, confirming that the ID-selected range preserves strong semantic matching capability.

D Benchmark Details

D.1 MTEB Benchmark

The Massive Text Embedding Benchmark (MTEB) (Muennighoff et al., 2023) provides a standardized framework for evaluating text

embeddings across diverse semantic scenarios. We conduct a comprehensive evaluation covering seven core task categories, encompassing 42 datasets to ensure a holistic assessment of semantic representations.

Semantic Textual Similarity (STS) Results are reported on the full suite of standard STS tasks, including BIOSSES, SICK-R, and STS12 through STS16. Following standard practice, we use the Spearman correlation between the cosine similarity of embedding pairs and human-annotated gold labels as the core metric for measuring fine-grained alignment in the embedding space.

Reranking and Retrieval Reranking performance is measured on AskUbuntuDupQuestions, MindSmallReranking, SciDocsRR, and StackOverflowDupQuestions using Mean Average Precision (MAP). For retrieval, we employ a broad set of benchmarks including NFCorpus, FiQA2018, SciFact, and QuoraRetrieval, where NDCG@10 serves as the primary metric for evaluating ranking effectiveness.

Classification and Summarization For classification tasks, we evaluate the discriminative capacity of embeddings on ToxicConversations, Imdb, Banking77, Emotion, and TweetSentimentExtraction, reporting the accuracy score for each. The summarization capability is measured via the SummEval dataset, where we calculate the Spearman correlation based on cosine similarity to evaluate the alignment between generated summaries and source documents.

Clustering and Pair Classification The clustering evaluation encompasses eleven datasets across diverse domains, including Biorxiv, Medrxiv, Reddit, and StackExchange, where performance is quantified using the V-measure. For pair classification tasks, such as TwitterURLCorpus and SprintDuplicateQuestions, we report Average Precision (AP) to measure the sensitivity of the model to binary semantic similarity.

D.2 LoCoV1 Benchmark

LoCoV1 (Saad-Falcon et al., 2024) serves as a specialized stress test for long-context stability. Unlike the predominantly short-form text in MTEB, LoCoV1 requires maintaining semantic density over extended sequences. To analyze the influence of sequence length on our KV re-routing mechanism,

we evaluate performance under controlled truncation at 1k, 2k, and 4k tokens. We adopt NDCG@10 for retrieval tasks, comparing the results against different baselines.

E Detailed MTEB Results

This section presents the detailed results for each task category in the MTEB benchmark (Muenninghoff et al., 2023). We report performance across three models: Qwen3-4B, Mistral-7B-Instruct-v0.1, and Llama-3.1-8B-Instruct. We compare six different embedding methods: Last Token, Mean Pooling, PromptEOL (Jiang et al., 2024), Echo (Springer et al., 2025), Token Prepending (Fu et al., 2025), and our proposed KV-Embedding.

The detailed breakdown of results is organized as follows. Table 8 reports the Spearman correlation scores for Semantic Textual Similarity (STS) tasks, while Table 9 details the Retrieval performance measured by NDCG@10. Classification accuracy across the evaluated datasets is shown in Table 10. For Pair Classification, Table 11 provides the Average Precision (AP) scores. Additionally, we present Clustering results measured by the Validity Measure (V-measure) in Table 12, Reranking performance (Mean Average Precision) in Table 13, and finally, the Summarization Spearman correlations in Table 14.

F Detailed LoCoV1 Results

The full results for LoCoV1 experiments are presented in Tables 15, 16, and 17. Across all three tested context windows and model architectures, our KV-Embedding method consistently achieves the highest average performance, demonstrating better robustness in long-context retrieval tasks.

G Attention Bias Experiment

During attention computation, we add a scalar bias b to the pre-softmax logit when attending to the re-routed KV pair at position 0. For a query \mathbf{q}_i at any position i , the modified attention score is:

$$\tilde{s}_{i,0} = \frac{\mathbf{q}_i^\top \mathbf{k}_0}{\sqrt{d}} + b \quad (5)$$

The final attention weights $\alpha_{i,j}$ are then computed as:

$$\alpha_{i,j} = \frac{\exp(\tilde{s}_{i,j})}{\sum_{k=0}^n \exp(\tilde{s}_{i,k})} \quad (6)$$

where $\tilde{s}_{i,k} = s_{i,k}$ for all $k > 0$. A higher b encourages stronger attention to the global summary.

Model	Method	Avg.	BIOSSES	SICK-R	STS12	STS13	STS14	STS15	STS16	STS-B
Qwen3-4B	Last Token	0.2818	0.2781	0.4939	0.1761	0.2796	0.1560	0.1161	0.4477	0.3068
	Mean Pooling	0.4571	0.5943	0.5148	0.4526	0.3556	0.3286	0.5481	0.5249	0.3378
	PromptEOL	0.6741	0.5997	0.6612	0.5428	0.7460	0.6356	0.7359	0.7541	0.7176
	Echo	0.6634	0.6726	0.6565	0.5796	0.6884	0.5972	0.7275	0.7246	0.6607
	Token Prepending	0.6370	0.5648	0.6405	0.5154	0.7040	0.6061	0.6947	0.6924	0.6785
	KV-Embedding	0.7141	0.7551	0.6835	0.6247	0.7740	0.6665	0.7622	0.7586	0.6887
Mistral-7B-Instruct-v0.1	Last Token	0.3915	0.3089	0.5465	0.2552	0.3657	0.2411	0.2488	0.6033	0.5629
	Mean Pooling	0.4885	0.6425	0.5036	0.3910	0.4536	0.3781	0.5854	0.5695	0.3843
	PromptEOL	0.6953	0.5817	0.6918	0.6554	0.7783	0.6740	0.7575	0.6981	0.7258
	Echo	0.7333	0.7716	0.7245	0.6041	0.7916	0.6822	0.7899	0.7581	0.7443
	Token Prepending	0.6775	0.5716	0.6825	0.6210	0.7587	0.6633	0.7343	0.6741	0.7145
	KV-Embedding	0.7720	0.7496	0.7683	0.6891	0.8056	0.7308	0.8254	0.7975	0.8097
Llama-3.1-8B-Instruct	Last Token	0.3513	0.3302	0.5315	0.1837	0.3846	0.2226	0.2052	0.5462	0.4063
	Mean Pooling	0.4702	0.6253	0.5103	0.3583	0.4200	0.3602	0.5650	0.5403	0.3824
	PromptEOL	0.6919	0.6509	0.7034	0.5765	0.7376	0.6306	0.7383	0.7636	0.7343
	Echo	0.7124	0.7704	0.6956	0.5428	0.7843	0.6514	0.7557	0.7676	0.7311
	Token Prepending	0.6968	0.6536	0.6959	0.5947	0.7642	0.6665	0.7416	0.7342	0.7240
	KV-Embedding	0.7398	0.7710	0.7254	0.6239	0.7793	0.6946	0.7819	0.7874	0.7546

Table 8: MTEB STS Spearman correlation results across different models and methods. The highest average score for each model is highlighted in bold.

Model	Method	Avg.	ArguAna	NFCorpus	FiQA	SciFact	SCIDOCs	Quora	TREC	Touche	CQADupstack
Qwen3-4B	Last Token	0.0722	0.0797	0.0175	0.0000	0.0087	0.0031	0.5140	0.0159	0.0000	0.0111
	Mean Pooling	0.0294	0.1674	0.0142	0.0047	0.0362	0.0034	0.0170	0.0193	0.0000	0.0021
	PromptEOL	0.1857	0.2462	0.0948	0.0519	0.2138	0.0850	0.6500	0.2393	0.0135	0.0767
	Echo	0.1727	0.2336	0.0347	0.0552	0.1146	0.0211	0.7465	0.2239	0.0327	0.0918
	Token Prepending	0.1622	0.1912	0.1060	0.0496	0.1294	0.0713	0.5622	0.1949	0.0066	0.1489
	KV-Embedding	0.2765	0.4643	0.1069	0.1023	0.4054	0.0608	0.6916	0.3957	0.0869	0.1749
Mistral-7B-Instruct-v0.1	Last Token	0.1036	0.0961	0.0347	0.0141	0.0220	0.0027	0.6655	0.0770	0.0022	0.0178
	Mean Pooling	0.0886	0.3972	0.0201	0.0095	0.2365	0.0044	0.0525	0.0669	0.0000	0.0100
	PromptEOL	0.1746	0.1030	0.1404	0.0781	0.2033	0.0934	0.5847	0.2212	0.0359	0.1118
	Echo	0.2414	0.2719	0.1199	0.0909	0.3325	0.0327	0.7676	0.3283	0.0487	0.1797
	Token Prepending	0.1619	0.0589	0.1453	0.0768	0.1838	0.0834	0.5520	0.2143	0.0173	0.1257
	KV-Embedding	0.3014	0.2543	0.2257	0.2063	0.3723	0.0969	0.7774	0.4387	0.1120	0.2292
Llama-3.1-8B-Instruct	Last Token	0.0887	0.1104	0.0210	0.0088	0.0136	0.0037	0.6128	0.0232	0.0007	0.0041
	Mean Pooling	0.0713	0.4113	0.0164	0.0023	0.1201	0.0030	0.0275	0.0593	0.0000	0.0017
	PromptEOL	0.2017	0.2983	0.1317	0.0747	0.2140	0.0740	0.6890	0.2316	0.0066	0.0957
	Echo	0.2941	0.3685	0.1183	0.1255	0.4756	0.0679	0.8026	0.4382	0.0581	0.1920
	Token Prepending	0.1817	0.0721	0.1893	0.0833	0.1678	0.1222	0.6488	0.1952	0.0131	0.1434
	KV-Embedding	0.3079	0.4965	0.2046	0.1507	0.4452	0.0724	0.7794	0.3993	0.0602	0.1629

Table 9: MTEB Retrieval (NDCG@10) results. The highest average score for each model is highlighted in bold. Abbreviations: *TREC* (TREC-COVID), *CQADupstack* (CQADupstackEnglishRetrieval).

Model	Method	Avg.	Toxic	Imdb	Banking77	Emotion	TweetSent
Qwen3-4B	Last Token	0.4243	0.6463	0.5616	0.1850	0.2636	0.4648
	Mean Pooling	0.4656	0.5867	0.6914	0.3730	0.2244	0.4527
	PromptEOL	0.6138	0.6976	0.7377	0.5057	0.5043	0.6236
	Echo	0.5761	0.6740	0.6315	0.6426	0.4049	0.5278
	Token Prepending	0.6283	0.6837	0.8281	0.4863	0.5079	0.6357
	KV-Embedding	0.6375	0.7088	0.7259	0.6746	0.4859	0.5922
Mistral-7B-Instruct-v0.1	Last Token	0.5314	0.6375	0.6324	0.5491	0.2958	0.5424
	Mean Pooling	0.5157	0.6180	0.7334	0.4702	0.2553	0.5019
	PromptEOL	0.6571	0.7202	0.8641	0.5416	0.5042	0.6554
	Echo	0.6398	0.6868	0.7290	0.7270	0.4452	0.6109
	Token Prepending	0.6580	0.7094	0.8654	0.5572	0.5034	0.6546
	KV-Embedding	0.6951	0.7101	0.8655	0.7204	0.5193	0.6602
Llama-3.1-8B-Instruct	Last Token	0.4769	0.6170	0.6163	0.3641	0.2753	0.5120
	Mean Pooling	0.4848	0.5940	0.7286	0.3796	0.2414	0.4801
	PromptEOL	0.6250	0.6880	0.8283	0.5530	0.4381	0.6179
	Echo	0.6261	0.6814	0.7328	0.6958	0.4418	0.5788
	Token Prepending	0.6577	0.7065	0.8926	0.5718	0.4796	0.6379
	KV-Embedding	0.6602	0.6931	0.8660	0.6876	0.4605	0.5939

Table 10: MTEB Classification (Accuracy) results. The highest average score for each model is highlighted in bold. Column headers are abbreviated: *Toxic* (ToxicConversations), *TweetSent* (TweetSentimentExtraction).

Model	Method	Avg.	TwitterURL	SprintDup	TwitSemEval
Qwen3-4B	Last Token	0.3054	0.4003	0.1278	0.3882
	Mean Pooling	0.5269	0.6720	0.5726	0.3361
	PromptEOL	0.5637	0.7592	0.3597	0.5722
	Echo	0.6367	0.6791	0.7071	0.5239
	Token Prepending	0.5206	0.7637	0.2008	0.5972
	KV-Embedding	0.6800	0.7898	0.7144	0.5357
Mistral-7B-Instruct-v0.1	Last Token	0.3440	0.4417	0.1441	0.4462
	Mean Pooling	0.5681	0.7388	0.5881	0.3774
	PromptEOL	0.5629	0.8079	0.1749	0.7059
	Echo	0.7560	0.8059	0.7916	0.6707
	Token Prepending	0.5764	0.8113	0.1974	0.7206
	KV-Embedding	0.7564	0.8460	0.6939	0.7291
Llama-3.1-8B-Instruct	Last Token	0.3554	0.4745	0.1289	0.4630
	Mean Pooling	0.5176	0.7157	0.4670	0.3701
	PromptEOL	0.5911	0.7624	0.3968	0.6140
	Echo	0.7125	0.7749	0.7314	0.6312
	Token Prepending	0.5734	0.7842	0.2385	0.6975
	KV-Embedding	0.7332	0.8161	0.7237	0.6598

Table 11: MTEB Pair Classification (Average Precision) results. The highest average score for each model is highlighted in bold. Column headers are abbreviated: *SprintDup* (SprintDuplicateQuestions), *TwitSemEval* (TwitterSemEval2015).

Model	Method	Avg.	BioP2P	BioS2S	MedP2P	MedS2S	Reddit	RedditP2P	StackEx	StackP2P	20News
Qwen3-4B	Last Token	0.2395	0.1783	0.1737	0.2059	0.2238	0.1610	0.3362	0.4269	0.3053	0.1441
	Mean Pooling	0.3305	0.3808	0.2528	0.3423	0.2806	0.1984	0.5372	0.4074	0.4088	0.1661
	PromptEOL	0.3651	0.2855	0.3095	0.2699	0.2989	0.3692	0.4943	0.5488	0.3500	0.3597
	Echo	0.3530	0.3290	0.2688	0.3085	0.2909	0.3228	0.4843	0.5631	0.3786	0.2306
	Token Prepending	0.3372	0.2851	0.3020	0.2681	0.3009	0.2799	0.4776	0.4002	0.3449	0.3757
	KV-Embedding	0.3903	0.3627	0.3165	0.2967	0.3181	0.3721	0.5526	0.5409	0.3890	0.3642
Mistral-7B-Instruct-v0.1	Last Token	0.2516	0.1043	0.1821	0.1824	0.2312	0.2666	0.3505	0.4848	0.2860	0.1766
	Mean Pooling	0.3472	0.3981	0.2696	0.3523	0.2889	0.2258	0.5847	0.4004	0.4078	0.1969
	PromptEOL	0.3158	0.2289	0.2779	0.2253	0.2671	0.3014	0.4622	0.4519	0.3301	0.2978
	Echo	0.3681	0.3407	0.2723	0.3183	0.2804	0.3496	0.5288	0.5566	0.3724	0.2942
	Token Prepending	0.2825	0.2124	0.2757	0.2156	0.2580	0.2173	0.4431	0.3192	0.3169	0.2841
	KV-Embedding	0.3902	0.3196	0.3308	0.2795	0.3107	0.3901	0.5538	0.5460	0.3685	0.4129
Llama-3.1-8B-Instruct	Last Token	0.2652	0.2125	0.1686	0.2169	0.2275	0.2741	0.3376	0.4912	0.2957	0.1630
	Mean Pooling	0.3577	0.4047	0.2820	0.3516	0.2860	0.2463	0.5870	0.4322	0.4237	0.2060
	PromptEOL	0.4035	0.3357	0.3406	0.2916	0.3291	0.4301	0.5354	0.5873	0.3543	0.4269
	Echo	0.4189	0.3574	0.3071	0.3303	0.3122	0.4419	0.5893	0.6279	0.4153	0.3891
	Token Prepending	0.3365	0.3037	0.3165	0.2672	0.3019	0.2847	0.4788	0.3781	0.3413	0.3559
	KV-Embedding	0.4448	0.3770	0.3654	0.3252	0.3453	0.4908	0.6061	0.6103	0.3992	0.4838

Table 12: MTEB Clustering (V-measure) results. The highest average score for each model is highlighted in bold. Column headers are abbreviated to fit the page (e.g., *BioP2P* for BiorxivClusteringP2P, *20News* for TwentyNews-groupsClustering).

Model	Method	Avg.	AskUbuntu	MindSmall	SciDocs	StackOverflow
Qwen3-4B	Last Token	0.3476	0.4255	0.2445	0.4790	0.2415
	Mean Pooling	0.3272	0.4378	0.2823	0.3543	0.2342
	PromptEOL	0.4924	0.5360	0.2947	0.7558	0.3833
	Echo	0.4315	0.5065	0.2791	0.5523	0.3880
	Token Prepending	0.4901	0.5263	0.2930	0.7573	0.3838
	KV-Embedding	0.5007	0.5672	0.3066	0.7203	0.4088
Mistral-7B-Instruct-v0.1	Last Token	0.3673	0.4432	0.2532	0.4964	0.2763
	Mean Pooling	0.3790	0.4760	0.2715	0.4777	0.2906
	PromptEOL	0.4835	0.5402	0.2905	0.7276	0.3759
	Echo	0.4751	0.5390	0.2863	0.6402	0.4347
	Token Prepending	0.4790	0.5403	0.2776	0.7120	0.3863
	KV-Embedding	0.5145	0.5723	0.3034	0.7533	0.4289
Llama-3.1-8B-Instruct	Last Token	0.3608	0.4447	0.2458	0.4866	0.2661
	Mean Pooling	0.3537	0.4510	0.2657	0.4254	0.2729
	PromptEOL	0.4991	0.5360	0.3095	0.7606	0.3902
	Echo	0.5074	0.5338	0.3147	0.7500	0.4313
	Token Prepending	0.4992	0.5533	0.2942	0.7458	0.4034
	KV-Embedding	0.5237	0.5612	0.3097	0.7841	0.4396

Table 13: MTEB Reranking (Mean Average Precision) results. The highest average score for each model is highlighted in bold. Column headers are abbreviated: *AskUbuntu* (AskUbuntuDupQuestions), *StackOverflow* (StackOverflowDupQuestions), *SciDocs* (SciDocsRR).

Model	Method	SummEval
Mistral-7B-Instruct-v0.1	Last Token	0.2823
	Mean Pooling	0.2557
	PromptEOL	0.2863
	Echo	0.2922
	Token Prepending	0.2921
Qwen3-4B	KV-Embedding	0.3088
	Last Token	0.2341
	Mean Pooling	0.1949
	PromptEOL	0.2396
	Echo	0.2294
Llama-3.1-8B-Instruct	Token Prepending	0.2483
	KV-Embedding	0.2566
	Last Token	0.2526
	Mean Pooling	0.1996
	PromptEOL	0.2788
Llama-3.1-8B-Instruct	Echo	0.2527
	Token Prepending	0.2880
	KV-Embedding	0.2796

Table 14: MTEB Summarization (Spearman correlation) results. The highest score for each model is highlighted in bold.

Table 18 shows the effect of varying b on MTEB performance. The improvement from $b = 0$ to $b = 1.0$ confirms that the re-routed KV pairs provide useful context for embedding quality. The performance curve remains stable across a wide range, fluctuating within $\pm 1.5\%$ (0.519 to 0.534), suggesting that the injected KV pairs integrate naturally with the pre-trained attention mechanism. However, performance decreases when b exceeds 3.0, indicating that excessive bias may cause over-reliance on the global summary at the expense of local details. We set $b = 1.0$ to balance global context access with local specificity.

H Geometry of the Embedding Space

To evaluate the structural properties of the representation space, we utilize the alignment and uniformity metrics proposed by Wang and Isola (2020). The metrics are computed on a subset of 1,000 sentence pairs from the F2LLM dataset (Zhang et al., 2025) using Mistral-7B-Instruct. Let $f(x) \in \mathbb{R}^d$ be the ℓ_2 -normalized embedding of sentence x .

Alignment Alignment evaluates the closeness of embeddings for semantically similar pairs. A lower alignment score indicates that the model effectively maps related instances to proximal regions in the latent space, preserving local semantic consistency:

$$\mathcal{L}_{\text{align}}(f; \alpha) \triangleq \mathbb{E}_{(x,y) \sim p_{\text{pos}}} [\|f(x) - f(y)\|_2^\alpha] \quad (7)$$

Following standard practice, we set $\alpha = 2$ in our experiments.

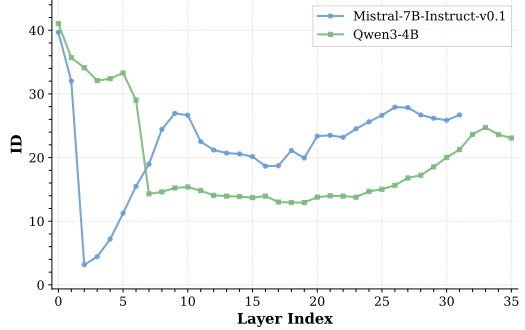


Figure 3: Intrinsic Dimensionality (ID) across layers for Mistral-7B-Instruct-v0.1 and Qwen3-4B. Different architectures exhibit distinct semantic compression patterns.

Uniformity Uniformity assesses how evenly embeddings are distributed across the unit hypersphere. High uniformity (a more negative score) suggests that the embeddings capture maximal information and avoid the *anisotropy* problem, where vectors collapse into a narrow cone:

$$\mathcal{L}_{\text{uniform}}(f; t) \triangleq \log \mathbb{E}_{x, y \stackrel{i.i.d.}{\sim} p_{\text{data}}} \left[e^{-t \|f(x) - f(y)\|_2^2} \right] \quad (8)$$

where $t = 2$ is used for evaluation. Together, these metrics provide a comprehensive view of the representation’s quality, balancing local clustering with global dispersion.

I Intrinsic Dimensionality Trajectories

Figure 3 presents the Intrinsic Dimensionality (ID) trajectories across all layers for Mistral-7B and Qwen3-4B. The ID is estimated using the TwoNN estimator (Facco et al., 2017) on 1,000 samples from the F2LLM dataset.

The visualization reveals distinct geometric patterns between the two architectures. Mistral-7B exhibits a sharp initial decline followed by fluctuations, with a stable low-ID region emerging around layers 13–19. Qwen3-4B demonstrates a more gradual descent, with its global ID minimum appearing around layers 17–19. In contrast, Qwen3-4B demonstrates a more gradual descent, with its global ID minimum appearing in the middle layers. Both models show a common trend where ID increases again as representations approach the final layers.

The variance in these trajectories indicates that the layers of maximal compression, where the representation manifold occupies the lowest number of intrinsic dimensions, differ by model. For Mistral-

Model	Method	2wiki mqa	court HTML	court Text	gov rep	legal case	multi qa	pass ret	qasper abs	qasper title	qmsum	stack over	summ scrn	Avg.
Mistral-7B	PromptEOL	0.0757	0.0020	0.0010	0.0059	0.0060	0.1515	0.0757	0.0047	0.0109	0.1492	0.0009	0.0134	0.0414
	Echo	0.1699	0.0034	0.0055	0.0047	0.0089	0.1515	0.1461	0.0703	0.0649	0.1033	0.0085	0.0151	0.0627
	Token Prepending	0.0757	0.0023	0.0023	0.0047	0.0059	0.1515	0.0757	0.0109	0.0109	0.1492	0.0028	0.0077	0.0416
	KV-Embedding	0.1983	0.0077	0.0090	0.2023	0.0163	0.6080	0.1656	0.1654	0.0338	0.3936	0.6191	0.1791	0.2165
Qwen3-4B	PromptEOL	0.0757	0.0045	0.0025	0.0000	0.0206	0.1515	0.0757	0.0109	0.0109	0.1289	0.0000	0.0144	0.0413
	Echo	0.3677	0.0106	0.0078	0.0047	0.0097	0.1515	0.0678	0.1034	0.2250	0.1673	0.0248	0.0134	0.0961
	Token Prepending	0.0674	0.0023	0.0023	0.0047	0.0059	0.1515	0.0757	0.0109	0.0109	0.1492	0.0029	0.0134	0.0414
	KV-Embedding	0.1155	0.0052	0.0087	0.0946	0.0125	0.3301	0.1221	0.0509	0.0187	0.2055	0.5391	0.0434	0.1289
Llama-3.1-8B	PromptEOL	0.0757	0.0045	0.0045	0.0044	0.0000	0.1515	0.0757	0.0099	0.0218	0.2012	0.0052	0.0009	0.0463
	Echo	0.1035	0.0186	0.0245	0.2445	0.0239	0.1515	0.0757	0.2633	0.3693	0.0436	0.0044	0.0304	0.1128
	Token Prepending	0.0757	0.0023	0.0023	0.0047	0.0059	0.1515	0.0757	0.0109	0.0109	0.1492	0.0029	0.0134	0.0421
	KV-Embedding	0.2357	0.0100	0.0184	0.3367	0.0206	0.4842	0.1985	0.1755	0.0436	0.2658	0.6868	0.1535	0.2191

Table 15: LoCoV1 Experimental Results: 1024 Token Length

Model	Method	2wiki mqa	court HTML	court Text	gov rep	legal case	multi qa	pass ret	qasper abs	qasper title	qmsum	stack over	summ scrn	Avg.
Mistral-7B	PromptEOL	0.1308	0.0023	0.0023	0.0047	0.0106	0.1515	0.0599	0.0148	0.0000	0.0955	0.0032	0.0134	0.0407
	Echo	0.1175	0.0051	0.0023	0.0047	0.0069	0.1973	0.0757	0.0109	0.0109	0.1181	0.0170	0.0160	0.0549
	Token Prepending	0.0757	0.0028	0.0023	0.0047	0.0059	0.1515	0.0757	0.0109	0.0109	0.1492	0.0029	0.0134	0.0422
	KV-Embedding	0.2246	0.0181	0.0197	0.1203	0.0266	0.4857	0.1307	0.0433	0.0415	0.3183	0.6072	0.1698	0.1838
Qwen3-4B	PromptEOL	0.0757	0.0015	0.0020	0.0073	0.0183	0.1515	0.0757	0.0070	0.0176	0.1492	0.0058	0.0134	0.0438
	Echo	0.3004	0.0055	0.0038	0.0047	0.0059	0.1515	0.0572	0.0109	0.0617	0.1033	0.0289	0.0556	0.0658
	Token Prepending	0.0757	0.0028	0.0023	0.0047	0.0059	0.1515	0.0757	0.0109	0.0109	0.1492	0.0029	0.0134	0.0422
	KV-Embedding	0.1387	0.0123	0.0166	0.0299	0.0319	0.2505	0.1203	0.0505	0.0419	0.1741	0.5090	0.0542	0.1192
Llama-3.1-8B	PromptEOL	0.0551	0.0006	0.0023	0.0047	0.0059	0.1515	0.0757	0.0109	0.0218	0.1492	0.0005	0.0143	0.0410
	Echo	0.0451	0.0012	0.0014	0.0058	0.0062	0.1515	0.0789	0.0171	0.0134	0.1035	0.0238	0.0141	0.0385
	Token Prepending	0.0757	0.0028	0.0023	0.0047	0.0059	0.1515	0.0757	0.0109	0.0109	0.1492	0.0029	0.0134	0.0422
	KV-Embedding	0.1591	0.0248	0.0355	0.1384	0.0552	0.4116	0.1237	0.0533	0.0433	0.3135	0.6733	0.1482	0.1817

Table 16: LoCoV1 Experimental Results: 2048 Token Length

Model	Method	2wiki mqa	court HTML	court Text	gov rep	legal case	multi qa	pass ret	qasper abs	qasper title	qmsum	stack over	summ scrn	Avg.
Mistral-7B	PromptEOL	0.0279	0.0023	0.0023	0.0051	0.0059	0.1816	0.1036	0.0133	0.0109	0.1649	0.0005	0.0123	0.0442
	Echo	0.1432	0.0023	0.0147	0.0063	0.0149	0.2289	0.0920	0.0055	0.0109	0.1534	0.0228	0.0147	0.0591
	Token Prepending	0.1097	0.0092	0.0133	0.0462	0.0709	0.2463	0.0771	0.1725	0.1611	0.1342	0.1327	0.0171	0.0992
	KV-Embedding	0.1626	0.0310	0.0416	0.0789	0.0794	0.3861	0.1058	0.3443	0.3061	0.2569	0.5945	0.0947	0.2068
Qwen3-4B	PromptEOL	0.0868	0.0137	0.0201	0.0689	0.0390	0.2347	0.0816	0.2283	0.2197	0.1202	0.3995	0.0307	0.1286
	Echo	0.1547	0.0096	0.0106	0.1195	0.0135	0.4423	0.1792	0.1291	0.0618	0.2233	0.1812	0.0564	0.1318
	Token Prepending	0.0790	0.0094	0.0212	0.0666	0.0323	0.2608	0.0968	0.2468	0.1953	0.2239	0.2436	0.0297	0.1255
	KV-Embedding	0.1118	0.0259	0.0369	0.0983	0.0964	0.3070	0.0952	0.4180	0.2973	0.1519	0.5003	0.0476	0.1822
Llama-3.1-8B	PromptEOL	0.1032	0.0121	0.0082	0.0852	0.0838	0.2628	0.0913	0.1678	0.1277	0.1383	0.4313	0.0306	0.1285
	Echo	0.1713	0.0036	0.0023	0.0047	0.0051	0.1515	0.0872	0.0081	0.0078	0.1242	0.4377	0.4263	0.1191
	Token Prepending	0.1233	0.0090	0.0084	0.0958	0.0579	0.2952	0.0989	0.2379	0.2285	0.1713	0.3247	0.0251	0.1397
	KV-Embedding	0.1685	0.0503	0.0552	0.1138	0.1360	0.3872	0.1369	0.4459	0.3751	0.2862	0.6730	0.0567	0.2404

Table 17: LoCoV1 Experimental Results: 4096 Token Length

Attention Bias	STS	Retr.	Class.	Pair.	Clust.	Rerank.	Summ.	Avg.
0.00	0.7690	0.2942	0.6948	0.7310	0.3855	0.5128	0.3096	0.5281
1.00	0.7720	0.3014	0.6951	0.7564	0.3902	0.5145	0.3088	0.5341
2.00	0.7736	0.3064	0.6949	0.7342	0.3926	0.5159	0.3107	0.5326
3.00	0.7723	0.3089	0.6938	0.7329	0.3928	0.5135	0.3100	0.5320
4.00	0.7649	0.3066	0.6907	0.7259	0.3928	0.5093	0.3027	0.5276
5.00	0.7483	0.2952	0.6819	0.7078	0.3875	0.5010	0.3110	0.5190

Table 18: Performance of Mistral-7B-Instruct with different attention bias values across various tasks.

7B, the minimum ID occurs very early, whereas for Qwen3-4B, it is situated in the middle of the backbone. These empirical observations justify the use of an automated selection strategy over a fixed layer heuristic, as the ID-based approach adaptively identifies the specific layers where information is most condensed for a given architecture.

J Analysis of Layer Selection

To validate the efficacy of Intrinsic Dimensionality (ID) for layer selection, we compare our strategy against uniform partitioning strategies: Early, Middle, and Late layers, each covering approximately one-third of the total model depth. As summarized in Table 19, re-routing layers \mathcal{L} derived from ID analysis consistently yield the highest average performance while maintaining a significantly more parsimonious selection of layers.

On Qwen3-4B, re-routing through early layers (0–11) results in the lowest average score (0.409). This supports the premise that shallow layers focus on surface-level lexical and syntactic features, which lack the semantic density required for effective global information redistribution. Conversely, ID selection identifies a specific range of layers (12–21) that achieves an average score of 0.494, outperforming the broader middle-third strategy (12–23).

A similar pattern emerges on Mistral-7B-Instruct-v0.1. On Mistral-7B, our ID-based selection utilizes only 7 layers (13–19) yet surpasses the 10-layer middle strategy (10–19). This efficiency indicates that minimum intrinsic dimensionality accurately pinpoints the layer range where the representation manifold achieves maximal compression. By injecting global context at these specific positions, our method avoids the noisy low-level features of early layers and the task-specific prediction bias inherent in final-layer hidden states. These findings suggest that semantic redistribution is most effective when applied at the stage of peak abstraction, rather than through uniform or heuristic selection.

K Impact of Attention Constraints

This section provides additional analysis on why naive mask removal fails, complementing the results in Table 4.

Decoder-only LLMs are pre-trained under strict causal constraints, where each token only attends to preceding positions. When bidirectional attention

is forced on a frozen model, every token suddenly receives key-value states from future positions that were never encountered during pre-training. These out-of-distribution states disrupt the learned attention patterns, causing the model to produce degraded representations.

The consistent performance collapse across both Qwen3-4B and Mistral-7B (Table 4) confirms that this is not a model-specific issue but a fundamental incompatibility between bidirectional attention and causally pre-trained weights. Notably, the degradation is most severe on Retrieval tasks, where Bi-Attn scores drop to near-zero (0.02–0.03), suggesting that document-level semantics are particularly disrupted.

KV-Embedding avoids this issue by operating within the causal framework. The re-routed KV states originate from the final token, which has legitimately attended to all preceding positions during the forward pass. By prepending these states rather than altering the attention mask, we preserve the model’s internal dynamics while enabling global context access.

L Prompt Design

Table 20 evaluates the impact of five different prompt variations on the performance of Mistral-7B-Instruct-v0.1. The results indicate that the model’s performance is consistent across different instruction phrasings, with the average scores ranging narrowly from 0.529 to 0.540. This stability suggests that the internal re-routing mechanism is robust to the specific choice of natural language instructions.

While the overall variance is minimal, specific templates exhibit localized advantages. For example, Prompt 0 (“Compress the context in one word”), which serves as our default configuration, achieves the highest scores in STS (0.772), Classification (0.695), and Summarization (0.309). This indicates its superior ability to capture global semantic information. On the other hand, Prompt 2 (“Extract key concept”) shows a slight edge in Retrieval (0.336) and Clustering (0.419), suggesting that phrasings emphasizing extraction may better align with task-specific representations for dense vector spaces.

M Pooling Strategy

Table 21 compares pooling strategies after KV re-routing. Mean pooling consistently performs worst

across all backbones. This likely reflects that early tokens retain lexical noise that averaging cannot filter, leading to semantic dilution even with re-routed context.

Hybrid pooling (averaging the last-token and mean representations) achieves the highest average scores. This strategy combines the distributive evidence across the sequence with the globally-informed summary captured by the final state.

Model	Layer Selection	STS	Retr.	Class.	Pair.	Clust.	Rerank.	Summ.	Avg.
Qwen3-4B	Early Layers (0–11)	0.527	0.253	0.578	0.470	0.362	0.441	0.234	0.409
	Middle Layers (12–23)	0.713	0.284	0.639	0.677	0.391	0.490	0.255	0.493
	Late Layers (24–35)	0.726	0.272	0.634	0.666	0.399	0.477	0.247	0.489
	ID Selected (12–21)	0.714	0.277	0.638	0.680	0.390	0.501	0.257	0.494
Mistral-7B-Instruct-v0.1	Early Layers (0–9)	0.759	0.277	0.691	0.732	0.381	0.505	0.301	0.521
	Middle Layers (10–19)	0.771	0.301	0.695	0.731	0.389	0.514	0.304	0.529
	Late Layers (20–31)	0.771	0.297	0.696	0.735	0.382	0.510	0.300	0.527
	ID Selected (13–19)	0.772	0.301	0.695	0.756	0.390	0.515	0.309	0.534

Table 19: Ablation study on layer selection. We compare uniform strategies (Early, Middle, Late) with ID-based selection (layer ranges shown in parentheses). ID selection achieves the best average performance while using fewer layers.

ID	Prompt Template	STS	Retr.	Class.	Pair.	Clust.	Rerank.	Summ.	Avg.
0	Compress the context in one word	0.772	0.301	0.695	0.756	0.390	0.515	0.309	0.534
1	Summarize in one word	0.768	0.292	0.683	0.756	0.391	0.518	0.303	0.530
2	Extract key concept	0.754	0.336	0.666	0.775	0.419	0.533	0.299	0.540
3	Represent in one word	0.766	0.294	0.683	0.755	0.392	0.517	0.299	0.529
4	Compress to one word	0.767	0.294	0.684	0.766	0.393	0.518	0.296	0.531

Table 20: Ablation on prompt templates (Mistral-7B). Performance is stable across prompts, with “Extract key concept” showing strength on retrieval and clustering tasks.

Model	Pooling Strategy	STS	Retr.	Class.	Pair.	Clust.	Rerank.	Summ.	Avg.
Qwen3-4B	Last Token	0.718	0.266	0.652	0.638	0.397	0.511	0.271	0.493
	Mean Pooling	0.504	0.177	0.516	0.535	0.351	0.411	0.219	0.388
	Hybrid Pooling	<u>0.714</u>	0.277	<u>0.638</u>	0.680	<u>0.390</u>	<u>0.501</u>	<u>0.257</u>	0.494
Mistral-7B-Instruct-v0.1	Last Token	0.767	0.253	0.694	0.683	0.338	0.503	0.292	0.504
	Mean Pooling	0.588	0.226	0.566	0.644	0.379	0.446	0.260	0.444
	Hybrid Pooling	0.772	0.301	0.695	0.756	0.390	0.515	0.309	0.534

Table 21: Ablation on pooling strategies. Hybrid pooling (last-token + mean) achieves the best overall performance. **Bold**: best, underline: second-best.